ORNL-TM-4196

THE DEVELOPMENT AND APPLICATION OF A DISCRETE ORDINATES ADJOINT DIFFERENCE METHOD FOR ONE-DIMENSIONAL SHIELD WEIGHT OPTIMIZATION

R. L. Childs
W. W. Engle, Jr.
J. C. Robinson
F. R. Mynatt

OAK RIDGE NATIONAL LABORATORY
OPERATED BY UNION CARBIDE CORPORATION • FOR THE U.S. ATOMIC ENERGY COMMISSION

DISCLAIMER

ORNL-TM-4196

Contract No. W-7405-eng-26

MATHEMATICS DIVISION

THE DEVELOPMENT AND APPLICATION OF A DISCRETE ORDINATES ADJOINT DIFFERENCE METHOD FOR ONE-DIMENSIONAL SHIELD WEIGHT OPTIMIZATION[a]

R. L. Childs J. C. Robinson[b]

W. W. Engle, Jr.[c] F. R. Mynatt[c]

a. Submitted to the University of Tennessee by R. L. Childs as a Master's Thesis in the Department of Nuclear Engineering

b. The University of Tennessee, Knoxville

c. Neutron Physics Division

JUNE 1973

NOTE:

This work performed for
NEUTRON PHYSICS DIVISION
and supported by
SPACE NUCLEAR SYSTEMS DIVISION
U. S. Atomic Energy Commission

OAK RIDGE NATIONAL LABORATORY
Oak Ridge, Tennessee 37830
operated by
UNION CARBIDE CORPORATION
for the
U. S. ATOMIC ENERGY COMMISSION

THIS PAGE

WAS INTENTIONALLY

LEFT BLANK

ABSTRACT

An improved method for the weight optimization of one-dimensional layered shields has been developed. The radiation transport problem is represented by coupled neutron-gamma ray discrete ordinates transport calculations. In the optimization procedure, forward and adjoint calculations are performed for the initial shield design. An approximate form of the perturbed adjoint is used in the adjoint difference approach to determine the effect of shield changes, and a simple closed form optimization algorithm is used as in the ASOP code.

Three realistic shield optimization problems were solved to demonstrate the capabilities of the method. A comparison between the results obtained using this method and the ASOP code showed the agreement of the two methods to be very good and the new method to be significantly faster.

TABLE OF CONTENTS

LIST OF TABLES

LIST OF FIGURES

CHAPTER I

INTRODUCTION

In many mobile reactor applications, system constraints require that the shield be minimum weight. For example, in space applications the high cost of launching a payload into earth orbit makes it necessary to minimize the weight of all components in the system. Thus, there is a need for analysis techniques which can be used to design minimum weight shields.

The shield optimization problem can be divided into two parts: the selection of the shielding materials, and the arrangement of these materials. Only the latter problem will be considered here. There are several different procedures that can be used to arrange shielding materials. One possible method is to let the shield be composed of several different materials whose volume fractions are continuous functions of position. However, there are disadvantages associated with a continuous distribution. In some cases, it is difficult, if not impossible, to fabricate a shield of this kind. Also, the benefit of self-shielding effects which can be gained by lumping a material is lost. Another method of arranging shielding materials is to divide the shield into regions in which the shielding material is homogeneous. The problem then is to find the optimal composition and optimal shape for each region. This work will be limited to the problem of one-dimensional shield weight optimization of layered shields in which the layer compositions are known.

I. PROBLEM STATEMENT

One purpose of a radiation shield is to reduce the radiation levels at all points outside the shield to acceptable values. For one-dimensional problems, there is often only one requirement: that the dose at the surface of the shield or at some point outside the shield not exceed a given value. For this case, the shield optimization problem can be stated mathematically as follows:

Assume a one-dimensional shield configuration that is uniquely defined by n variables. Let a vector $\overline{X}$ be defined in n-dimensional vector space with the n variables as components. Possible choices for the variables are such things as layer thicknesses, boundary positions, or any other quantities that completely specify the configuration. The problem is then to find a vector $\overline{X}_0$ such that the function $W(\overline{X})$ is minimized at $\overline{X}_0$ subject to the condition that $D(\overline{X}_0)$ equal the dose constraint. Here $W(\overline{X})$ denotes the shield weight, and $D(\overline{X})$ denotes the dose at some point outside or at the surface of the shield.

II. PRESENTLY AVAILABLE METHODS

One method currently in use for the design of minimum weight, layered radiation shields is the method of steepest descent (1, 2, 3, 4). This method is an iterative procedure which can be summarized as follows:

1. Choose an initial vector $\overline{X}_1$ such that

$$D(\overline{X}_1) = D_c, \tag{1-1}$$

where D_c is the dose constraint.

2. Find a unit vector $\overline{\delta X}$ which points in the direction of maximum allowable decrease in $W(\overline{X})$ subject to the constraint that $\overline{\delta X}$ be tangent to the surface

$$D(\overline{X}) = D_c. \tag{1-2}$$

3. Calculate a new vector $\overline{X}_2$ defined by

$$\overline{X}_2 = \overline{X}_1 + \lambda\overline{\delta X} \tag{1-3}$$

where λ is an arbitrary iteration parameter.

4. Calculate a corrected point $\overline{X}_2$ such that the dose constraint is met. The definition of the vector $\overline{\delta X}$ causes this correction to be small.

5. Set $\overline{X}_1$ equal to $\overline{X}_2$ and repeat steps 2. through 5. until some convergence criterion is satisfied.

Summarizing, the method of steepest descent is an iterative procedure which starts with an initial shield configuration that satisfies the dose constraint and iteratively changes the configuration, following a constant-dose, decreasing-weight path, until a minimum weight configuration is found. The quantities $\nabla D(\overline{X}_1)$ and $\nabla W(\overline{X}_1)$ are required to calculate the vector $\overline{\delta X}$. At each point in the iterative scheme, the dose, the weight, and their gradients are required, and the information obtained is a vector which tells the direction in which to move but not how far to move.

Another method that has been used to solve constrained function minimization problems is the method of LaGrange multipliers (5). One way to obtain this result is to minimize a new function defined by

$$H(\bar{X}, \lambda) = W(\bar{X}) + \lambda[D(\bar{X}) - D_c]. \tag{1-4}$$

The function H will have a stationary value provided

$$\frac{\partial H}{\partial X_i} = 0, \qquad i = 1 \text{ to } n, \tag{1-5}$$

$$\text{and } \frac{\partial H}{\partial \lambda} = 0.$$

These requirements may be written as

$$\frac{\partial W}{\partial X_i} + \lambda \frac{\partial D}{\partial X_i} = 0, \qquad i = 1 \text{ to } n, \tag{1-6}$$

$$\text{and } D(\bar{X}) - D_c = 0.$$

The last requirement implies that the constraint is satisfied and that H equals W.

Clark and Kam (5), solve Equations (1-6) by expanding every function in a first order Taylor expansion and replacing λ with $\lambda_o + \delta\lambda$. By ignoring products of incrementals, the system of equations becomes a set of n + 1 linear equations with n + 1 unknowns which is solved for $\overline{\delta X}$ and $\delta\lambda$. These results are used to obtain new guesses for $\bar{X}$ and λ and the process is repeated until convergence is obtained.

Thus, the numerical implementation of the method of LaGrange multipliers is an iterative procedure which requires an initial guess for $\bar{X}$ and λ and uses a linear approximation to obtain successive estimates of $\bar{X}$ and λ until a stationary point is found. The information required at

each step in the iteration is:

$$D(\bar{X}),\ W(\bar{X}),\ \frac{\partial D(\bar{X})}{\partial X_i},\ \frac{\partial W(\bar{X})}{\partial X_i},\ \frac{\partial^2 D(\bar{X})}{\partial X_i \partial X_j},\ \text{and}\ \frac{\partial^2 W(\bar{X})}{\partial X_i \partial X_j}\ \text{for } i = 1 \text{ to } n,\ j = 1 \text{ to } n.$$

The information obtained is a new estimate of the optimal shield configuration.

The main difficulty in applying the method of steepest descent, the method of LaGrange multipliers, or any other numerical function minimization algorithm to the problem of shield weight optimization is evaluating the dose and its derivatives. The rigorous way to calculate the dose is to solve the transport equation. However, since transport calculations are relatively time consuming, and a large number of dose evaluations are required to obtain the required derivatives, transport calculations are not used directly in the optimization process in most presently available methods (2, 3, 6). Instead, simplified models are used to relate the dose to the thicknesses of the materials present. Mynatt (7) observed that the complexity of the transport problem for a high-efficiency shield requires that a rigorous method be used for the transport portion of the shield optimization problem even if this precludes the use of attractive optimization techniques. Engle and Mynatt (8) have developed a computer program called ASOP (9) which incorporates discrete ordinates transport calculations directly into the optimization process.

The optimization technique used in ASOP is based upon the following assumptions:

1. The dose can be approximated by an exponential of the form

$$D(\bar{X}_0 + \overline{\delta X}) \cong D(\bar{X}_0)\ \exp[\sum_i A_i\ \delta X_i], \tag{1-7}$$

where A_i is a constant. This approximation is based on the observation that the attenuation of radiation is roughly exponential in nature.

2. The dose-weight derivatives can be approximated by a truncated Taylor series of the form

$$\frac{\partial D}{\partial W}\Big|_{X_i}^{O} + \delta X_i = \frac{\partial D}{\partial W}\Big|_{X_i}^{O} + \left[\frac{\partial}{\partial X_i}\left(\frac{\partial D}{\partial W}\right)\right]_{X_i}^{O} \delta X_i\ , \tag{1-8}$$

where $$\frac{\partial D}{\partial W} \equiv \frac{\partial D}{\partial X_i}\Big/\frac{\partial W}{\partial X_i}\ .$$

These approximations are valid for small values of δX_i, and use of the ASOP program has shown that they are fairly accurate for moderate sized changes.

From the method of LaGrange multipliers (see Equation (1-6)) a necessary condition for a minimum weight shield is that the dose-weight derivatives be equal. Requiring that the dose equal the dose constraint and that the dose-weight derivatives be equal yields the following n + 1 linear equations:

$$\sum_i A_i\ \delta X_i = \ell n\left(\frac{D_c}{D(\bar{X}_0)}\right) \tag{1-9}$$

and

$$\left[\frac{\partial}{\partial X_i}\left(\frac{\partial D}{\partial W}\right)\right]_{X_i}^{O} \delta X_i - \lambda' = -\frac{\partial D}{\partial W}\Big|_{X_i}^{O},\ i = 1 \text{ to } N, \tag{1-10}$$

where λ' is the dose-weight derivative.

These equations contain n + 1 unknowns, the δX_i's and λ, and are easily solved once the constant terms are evaluated. ASOP evaluates the constants by performing a series of ANISN(10) calculations which consist of the initial configuration and two displacements of each movable boundary. Finite difference equations are then used to evaluate the constant terms.

The set of linear equations can be solved by multiplying each Equation (1-10) by $A_i/[\frac{\partial}{\partial X_i}(\frac{\partial D}{\partial W})]_{X_i^0}$ and subtracting from Equation (1-9). The result is

$$\lambda' = \frac{\ell n(D_c/D(\bar{X}_0)) + \sum_i \frac{A_i \frac{\partial D}{\partial W}\Big|_{X_i^0}}{[\frac{\partial}{\partial X_i}(\frac{\partial D}{\partial W})]_{X_i^0}}}{\sum_i \frac{A_i}{[\frac{\partial}{\partial X_i}(\frac{\partial D}{\partial W})]_{X_i^0}}} \qquad (1\text{-}11)$$

Once λ' is known, Equation (1-10) can be solved for δX_i.

The procedure used in ASOP is to solve for the δX_i's and use them to update the vector $\bar{X}_0$. The series of ANISN calculations is then repeated and the iteration is continued until both the dose and the dose-weight derivatives converge. In each step of the iteration, 2n + 1 ANISN calculations are required to obtain a new estimate of the minimum weight configuration.

III. PURPOSE

The purpose of this work is to develop a new method for calculating minimum weight shields. Most methods used for shield weight optimization use highly simplified calculational models to represent

the radiation transport in the shield. However, since these simple models are not based on a rigorous solution of the transport problem, they introduce errors into the optimization process, and it is difficult to estimate the magnitude of these errors. The ASOP method is based on transport calculations but has other deficiencies. A large number of transport calculations are required to obtain a minimum weight shield. This makes ASOP calculations costly and tends to limit the amount of detail which may be included in the transport calculation. For example, the use of relatively few energy groups may tend to distort important details of the radiation transport. Also the ASOP method does not allow the use of general function minimization algorithms which are available. The approach to be used in this development is to obtain a simplified function to describe the variation of dose with changes of the shield configuration which is based on a rigorous solution of the transport problem. This approach allows the use of general minimization techniques. By using certain properties of adjoint transport theory, the function can be obtained using the results from two transport calculations, one forward and one adjoint. Since the ASOP technique requires $2n + 1$ calculations, the new method should require significantly less computer time.

CHAPTER II

DEVELOPMENT OF THE CALCULATIONAL METHOD

In this chapter, the techniques to be used in calculating optimum shield configurations are developed. The theoretical concepts utilized and the approximations made to obtain a simplified dose-thickness relationship are presented. Finally, the optimization procedure to be used is described.

I. THE DIFFERENCE FLUX FORMULATION

The Boltzmann transport equation describes mathematically the behavior of neutrons or photons in terms of seven-dimensional phase space. The form often of interest in shielding applications is the time-independent form given by

$$\nabla\cdot\bar{\Omega}\Phi(\bar{r},E,\bar{\Omega}) + \Sigma_t(\bar{r},E)\,\Phi(\bar{r},E,\bar{\Omega}) = S(\bar{r},E,\bar{\Omega})$$

$$+\int\int\Sigma_s(\bar{r},E'\rightarrow E,\bar{\Omega}'\rightarrow\bar{\Omega})\,\Phi(\bar{r},E',\bar{\Omega}')\,dE'\,d\bar{\Omega}', \qquad (2\text{-}1)$$

where

$\Phi(\bar{r},E,\bar{\Omega})$ = the particle flux at position $\bar{r}$, energy E, and direction $\bar{\Omega}$ per unit energy per unit solid angle;

$\Sigma_t(\bar{r},E)$ = the total macroscopic cross section at position $\bar{r}$, and energy E;

$\Sigma_s(\bar{r},E'\rightarrow E,\bar{\Omega}'\rightarrow\bar{\Omega})$ = the macroscopic differential scattering cross section for particles with initial energy E' and direction $\bar{\Omega}'$ which scatter at

position $\bar{r}$ and emerge with energy E and direction $\bar{\Omega}$ per unit energy per unit solid angle;

$S(\bar{r},E,\bar{\Omega})$ = source particles emitted at $\bar{r}$ with energy E and direction $\bar{\Omega}$ per unit energy per unit solid angle per unit volume.

In order to simplify notation, it is convenient to write Equation (2-1) in operator notation as

$$\hat{H}\Phi(\bar{P}) = S(\bar{P}), \tag{2-2}$$

where $\bar{P}$ represents position, energy, and direction phase space.

In the shield optimization problem, a reference shield configuration and several arbitrary perturbations of that shield configuration will be considered. It is convenient to relate the perturbed flux to the unperturbed flux as follows:

$$\Phi(\bar{P}) = \Phi_0(\bar{P}) + \delta\Phi(\bar{P}), \tag{2-3}$$

where the subscript zero denotes the unperturbed or reference configuration, and $\delta\Phi(\bar{P})$ is called the difference flux (11, 12, 13, 14).

Substituting Equation (2-3) into Equation (2-2) gives:

$$\hat{H}[\Phi_0(\bar{P}) + \delta\Phi(\bar{P})] = S(\bar{P}). \tag{2-4}$$

Since the Boltzmann operator is linear (15), Equation (2-4) can be written as

$$\hat{H}\Phi_0(\bar{P}) + \hat{H}\delta\Phi(\bar{P}) = S(\bar{P}). \tag{2-5}$$

The Boltzmann equation for the unperturbed case is

$$\hat{H}_0\Phi_0(\bar{P}) = S(\bar{P}). \tag{2-6}$$

Subtracting Equation (2-6) from Equation (2-5) and rearranging terms yields:

$$\hat{H}\delta\Phi(\bar{P}) = [\hat{H}_0 - \hat{H}]\ \Phi_0(\bar{P}). \tag{2-7}$$

Equation (2-7) may be written as

$$\hat{H}\delta\Phi(\bar{P}) = f(\bar{P}), \tag{2-8}$$

where

$$f(\bar{P}) \equiv [\hat{H}_0 - \hat{H}]\ \Phi_0(\bar{P}). \tag{2-9}$$

The effects of perturbations can be evaluated by solving Equation (2-8). However, most presently available computer programs could not be used because the source term $f(\bar{P})$ is positive in some regions of phase space and negative in others.

II. ADJOINT TRANSPORT CALCULATIONS

Transport problems that have a single source and many detectors can be solved by a single, forward transport calculation. However, transport problems that have several different sources and a single detector would require a separate, forward transport calculation for each source. Problems of this type can be solved more efficiently using adjoint transport theory.

The adjoint of the operator $\hat{H}$ is defined as an operator, $\hat{H}^+$, that satisfies the following equation:

$$\int_{\bar{P}_0} \Phi^+(\bar{P})\, \hat{H}\Phi(\bar{P})\, d\bar{p} = \int_{\bar{P}_0} \Phi(\bar{P})\, \hat{H}^+\Phi^+(\bar{P})\, d\bar{p} + \text{B. T.}, \tag{2-10}$$

where

B. T. is a boundary term;

$\bar{P}_0$ is a region of phase space that includes a volume, V_0, all energies, and all directions;

and $\Phi(\bar{P})$ and $\Phi^+(\bar{P})$ are any functions that satisfy certain boundary and continuity conditions (16).

When $\hat{H}$ is the operator defined in Equations (2-1) and (2-2), $\hat{H}^+$ is given by the following equation (16):

$$\hat{H}^+\Phi^+(\bar{P}) = -\nabla\cdot\bar{\Omega}\Phi^+(\bar{r},E,\bar{\Omega}) + \Sigma_t(\bar{r},E)\, \Phi^+(\bar{r},E,\bar{\Omega})$$

$$-\int\int \Sigma_s(\bar{r},E\rightarrow E',\vec{\Omega}\rightarrow\vec{\Omega}')\, \Phi^+(\bar{r},E',\bar{\Omega}')\, dE'd\bar{\Omega}'. \tag{2-11}$$

The only boundary term comes from the first term in the $\hat{H}$ operator and

is as follows (16):

$$B.\ T. = \iiint_{S_0} (\bar{n}\cdot\bar{\Omega})\ \Phi(\bar{P})\ \Phi^{+}(\bar{P})\ dSdEd\bar{\Omega}, \tag{2-12}$$

where S_0 is the surface of the volume V_0. Let the functions $\Phi(\bar{P})$ and $\Phi^{+}(\bar{P})$ be defined by the following equations:

$$\hat{H}\Phi(\bar{P}) = S(\bar{P}) \tag{2-13}$$

and

$$\hat{H}^{+}\Phi^{+}(\bar{P}) = R(\bar{P}), \tag{2-14}$$

where $R(\bar{P})$ is any response function. If Equation (2-13) is multiplied by $\Phi^{+}(\bar{P})$, Equation (2-14) is multiplied by $\Phi(\bar{P})$, and the resulting expressions are subtracted and integrated over $\bar{P}_0$, the following result is obtained:

$$\int_{\bar{P}_0} \Phi^{+}(\bar{P})\ \hat{H}\Phi(\bar{P})\ d\bar{P} - \int_{\bar{P}_0} \Phi(\bar{P})\ \hat{H}^{+}\Phi^{+}(\bar{P})\ d\bar{P} =$$

$$\int_{\bar{P}_0} \Phi^{+}(\bar{P})\ S(\bar{P})\ d\bar{P} - \int_{\bar{P}_0} \Phi(\bar{P})\ R(\bar{P})\ d\bar{P}. \tag{2-15}$$

Substituting Equations (2-10) and (2-12) into Equation (2-15) and rearranging terms yields the following result:

$$\int_{\bar{P}_0} \Phi(\bar{P})\ R(\bar{P})\ d\bar{P} = \int_{\bar{P}_0} \Phi^{+}(\bar{P})\ S(\bar{P})\ dP$$

$$- \iiint_{S_0} (\bar{n}\cdot\bar{\Omega})\ \Phi(\bar{P})\ \Phi^{+}(\bar{P})\ dSdEd\bar{\Omega}. \tag{2-16}$$

Equations (2-13) and (2-14) do not uniquely define $\Phi(\bar{P})$ and $\Phi^{+}(\bar{P})$

because boundary conditions have not been specified. If the surface S_o is chosen to be a nonreentrant surface that envelops the outer surface of the system, no particles enter the surface of the system. Thus, the boundary condition is:

$$\Phi(\bar{r}_s, E, \bar{\Omega}) = 0, \text{ for } (\bar{n}\cdot\bar{\Omega}) < 0. \tag{2-17}$$

Equation (2-16) is valid no matter what boundary condition is chosen for $\Phi^+(\bar{P})$. The boundary term in Equation (2-16) may be eliminated by choosing the following boundary condition:

$$\Phi^+(\bar{r}_s, E, \bar{\Omega}) = 0, \ (\bar{n}\cdot\bar{\Omega}) > 0. \tag{2-18}$$

Equation (2-16) thus becomes

$$\int_{\bar{P}_0} \Phi(\bar{P})\, R(\bar{P})\, d\bar{P} - \int_{\bar{P}_0} \Phi^+(\bar{P})\, S(\bar{P})\, d\bar{P}. \tag{2-19}$$

The boundary condition chosen for $\Phi^+(\bar{P})$ is consistent with the interpretation of $\Phi^+(\bar{P})$ as an importance function (16). This is easily demonstrated by considering the special situation where $S(\bar{P})$ is a unit point source in phase space given by

$$S(\bar{P}) = \delta(\bar{r} - \bar{r}_0)\, \delta(\bar{\Omega} - \bar{\Omega}_0)\, \delta(E - E_0). \tag{2-20}$$

For this case, Equation (2-19) becomes

$$\Phi^+(r_0, E_0, \bar{\Omega}_0) = \int_{\bar{P}_0} \Phi(\bar{P})\, R(\bar{P})\, d\bar{P}. \tag{2-21}$$

Thus, $\Phi^+(\bar{P})$ is the probable contribution of a particle at $\bar{P}$ to the response.

The left hand side of Equation (2-19) represents the way to calculate a response of some type using values of $\Phi(\bar{P})$ obtained from a forward calculation. The right hand side of Equation (2-19) may be used to calculate the same result using values of $\Phi^+(\bar{P})$ obtained from an adjoint calculation. The adjoint method (using $\Phi^+(\bar{P})$) allows problems with many different sources and a single detector to be solved using the results of single transport calculation.

III. AN APPROXIMATE DOSE-THICKNESS RELATIONSHIP

The relationship between the dose at a given point and the flux can be expressed as follows

$$D = \int_{\bar{P}_0} \Phi(\bar{P})\, R(\bar{P})\, d\bar{P}. \tag{2-22}$$

For a point quantity such as dose, the spatial dependence of $R(\bar{P})$ is represented by a delta function. Substituting Equation (2-3) into Equation (2-22) yields:

$$\begin{aligned} D &= \int_{\bar{P}_0} \Phi_0(\bar{P})\, R(\bar{P})\, d\bar{P} + \int_{\bar{P}_0} \delta\Phi(\bar{P})\, R(\bar{P})\, d\bar{P} \\ &= D_0 + \int_{\bar{P}_0} \delta\Phi(\bar{P})\, R(\bar{P})\, d\bar{P}, \end{aligned} \tag{2-23}$$

where D_0 is the dose in the unperturbed case. Equation (2-8) is the Boltzmann equation for the difference flux, and Equation (2-19) is an

alternate expression for integrals like the one in Equation (2-23). Using Equations (2-8) and (2-19), Equation (2-23) may be written as

$$D = D_0 + \int_{\bar{P}_0} \Phi^+(\bar{P})\, f(\bar{P})\, d\bar{P}. \tag{2-24}$$

This result is sometimes called the adjoint difference method (12, 14).

The objective of this development is to obtain an expression for D which is accurate for any small perturbation and can also be easily evaluated for a large number of different perturbations. Equation (2-23) is not suitable for this purpose because $\delta\Phi(\bar{P})$ is different for each perturbation. Equation (2-24) can be used provided suitable expressions for $\Phi^+(\bar{P})$ and $f(\bar{P})$ can be found. For small perturbations, $\Phi_0^+(\bar{P})$ is a good approximation for $\Phi^+(\bar{P})$. The equivalent source was defined in Equation (2-9) using operator notation. Equation (2-9) can be written as:

$$f(\bar{r},E,\bar{\Omega}) = \iint[\Sigma_s(\bar{r},E'\to E,\bar{\Omega}'\to\bar{\Omega}) - \Sigma_s^0(\bar{r},E'\to E,\bar{\Omega}'\to\bar{\Omega})]\, \Phi_0(\bar{r},E',\bar{\Omega}')\, dE'd\bar{\Omega}'$$

$$- [\Sigma_t(\bar{r},E) - \Sigma_t^0(r,E)]\, \Phi_0(\bar{r},E,\bar{\Omega}). \tag{2-25}$$

In one-dimensional geometries, Equation (2-25) can be further simplified provided the perturbations considered are limited to changes in zone thicknesses. In this case, a given fractional change in zone thickness can be approximated by the same fractional change in the density of the zone. This relationship is exact for slab geometry but is only an approximation in cylindrical and spherical geometries because of curvature effects. Using this approximation, the perturbed cross sections are

$$\Sigma_s(\bar{r},E'\to E,\bar{\Omega}'\to\bar{\Omega}) = \frac{\rho(\bar{r})}{\rho_0(\bar{r})}\,\Sigma_s^0(\bar{r},E'\to E,\bar{\Omega}'\to\bar{\Omega}) \tag{2-26}$$

and

$$\Sigma_t(\bar{r},E) = \frac{\rho(\bar{r})}{\rho_0(\bar{r})}\,\Sigma_t^0(\bar{r},E), \tag{2-27}$$

where $\rho(\bar{r})$ is the "density" at position $\bar{r}$.

Substituting these expressions into Equation (2-25) yields

$$f(\bar{r},E,\bar{\Omega}) = \left(\frac{\rho(\bar{r})}{\rho_0(\bar{r})} - 1\right)\left[\iint\Sigma_s^0(\bar{r},E'\to E,\bar{\Omega}'\to\bar{\Omega})\;\Phi_0(\bar{r},E',\bar{\Omega}')\;dE'\,d\bar{\Omega}'\right.$$

$$\left. - \Sigma_t^0(\bar{r},E)\;\Phi_0(\bar{r},E,\bar{\Omega})\right]. \tag{2-28}$$

Note that the term in the brackets depends only on the unperturbed conditions. Equation (2-28) can be written as

$$f(\bar{r},E,\bar{\Omega}) = \left(\frac{\rho(\bar{r})}{\rho_0(\bar{r})} - 1\right)\,f_0(\bar{r},E,\bar{\Omega}), \tag{2-29}$$

where $f_0(\bar{r},E,\bar{\Omega})$ is the term in the bracket in Equation (2-28). Substituting Equation (2-29) into Equation (2-24) gives

$$D = D_0 + \int_{\bar{P}_0}\Phi^+(\bar{P})\left(\frac{\rho(\bar{r})}{\rho_0(\bar{r})} - 1\right)\,f_0(\bar{P})\;d\bar{P}. \tag{2-30}$$

If the perturbation is a uniform change in density in one zone in which $\rho_0(\bar{r})$ is constant, Equation (2-30) becomes

$$\Delta D_i = \frac{\Delta \rho_i}{\rho_{0_i}} \int_{\bar{Z}_i} \Phi^+(\bar{P})\, f_0(\bar{P})\, d\bar{P}, \tag{2-31}$$

where $\bar{Z}_i$ is the zone where the perturbation was introduced. Dividing Equation (2-31) by $\Delta\rho_i$ and taking the limit as $\Delta\rho_i$ approaches zero yields

$$\frac{\partial D}{\partial \rho_i}\Big|_0 = \frac{1}{\rho_{0_i}} \int_{\bar{Z}_i} \Phi_0^+(\bar{P})\, f_0(\bar{P})\, d\bar{P}. \tag{2-32}$$

It was shown in Chapter I that a necessary condition for a multizone shield to be minimum weight is that all dose-weight derivatives be equal. The dose-weight derivatives can be evaluated as follows:

$$\frac{\partial D}{\partial W} = \frac{\partial D}{\partial X_i} \Big/ \frac{\partial W}{\partial X_i} = \left(\sum_{j=1}^{N} \frac{\partial D}{\partial \rho_j} \frac{\partial \rho_j}{\partial X_i}\right) \Big/ \frac{\partial W}{\partial X_i}. \tag{2-33}$$

Thus, Equations (2-32) and (2-33) can be used to determine if a shield meets the necessary condition. Also, Equations (2-32) and (2-33) provide the information necessary to apply the method of steepest descent. However, the method of steepest descent requires that D_0 equal the dose constraint and does not give any information about the magnitude of the change to be made to the configuration. For these reasons, it is desirable to use the more general relationship, Equation (2-31), instead of Equation (2-32) in the optimization procedure.

In order to use Equation (2-31), the perturbed adjoint flux, $\Phi^+(\bar{P})$ is required. Since it is not practical to obtain $\Phi^+(\bar{P})$ rigorously,

a simple approximation is used to obtain a relationship between $\Phi^+(\bar{P})$ and $\Phi_0^+(\bar{P})$. Physically, $\Phi^+(\bar{P})$ is the contribution of a particle at point $\bar{P}$ to the dose. The effect of an increase in density (or zone thickness) is to place additional material between the particle and the detector. Thus, the amount of material between the particle and the detector in the perturbed case is identical to the amount of material between another point farther from the detector and the detector in the unperturbed case. Therefore, a simple approximation for $\Phi^+(\bar{P})$ is $\Phi_0^+(\bar{P}')$ where $\bar{P}'$ is the second point. Semi-log plots of the importance of particles in one-dimensional shields to the dose at the surface of the shield show that the variation of importance with position can be well represented by a single exponential in any homogeneous zone. (The path length stretching used in Monte Carlo calculations (17) is based on this observation.) Using the two approximations just mentioned, the perturbed adjoint flux (importance) is

$$\Phi^+(\bar{P}) \simeq \Phi_0^+(\bar{P}) \exp\left[- (r_b^i - r) \left(\frac{\rho_i}{\rho_0} - 1\right) \overline{\frac{\partial \ell n \Phi_0^+(\bar{P})}{\partial r}} \right], \qquad (2\text{-}34)$$

where r_b^i is the boundary of the zone nearest to the detector (the right boundary) and $\overline{\frac{\partial \ell n \Phi_0^+(\bar{P})}{\partial r}}$ is the average logarithmic slope of $\Phi_0^+(\bar{P})$ in the zone. A case where this approximation can fail is when particles farther from the detector are more important than particles closer to the detector. An example of this is the importance of low energy neutrons in a hydrogenous zone adjacent to a heavy metal zone. The

contribution of these neutrons to the neutron dose at the surface of the shield is negligibly small. However, these neutrons can enter the heavy metal region and produce secondary gamma rays which can contribute to the total dose. For these neutrons, Equation (2-34) predicts that their importance grows exponentially with increasing density. This is a nonphysical result which could make Equation (2-34) a very poor approximation, even if this phenomenon occurs only in a few relatively unimportant regions of phase space. Physically, the heavy metal appears to be a "detector" to the neutrons. Thus, Equation (2-34) can still be used provided r_b^i is replaced by $r_b^i(\bar{P})$, where $r_b^i(\bar{P})$ is defined to be the boundary where the importance is larger for a given neutron energy and direction. Equation (2-34) then becomes

$$\Phi^+(\bar{P}) = \Phi_0^+(\bar{P}) \exp\left[- (r_b^i(P) - r) \left(\frac{\rho_i}{\rho_i} - 1\right) \overline{\frac{\partial \ell n \Phi_0^+(\bar{P})}{\partial r}}\right], \qquad (2\text{-}35)$$

where $r_b^i(\bar{P}) \equiv$ the right boundary of the zone if $\overline{\frac{\partial \ell n \Phi_0^+(\bar{P})}{\partial r}} \geq 0$,

the left boundary of the zone if $\overline{\frac{\partial \ell n \Phi_0^+(\bar{P})}{\partial r}} < 0$.

Equation (2-35) insures that importance decreases whenever the density increases which is more realistic than Equation (2-34). Equation (2-35) was used in the calculations described in Chapter IV.

Consider a point isotropic monoenergetic source enclosed by several concentric shells of shielding material. The uncollided flux at a point outside the shield is:

$$\Phi_u = \Phi_0 e^{-\sum_i \Sigma_t^i t_i} \tag{2-36}$$

where Φ_0 is the flux when no shielding material is present,

Σ_t^i is the total cross section of the ith material,

and t_i is the thickness of the ith shell.

Equation (2-36) can also be written as

$$\Phi_u = \Phi_0 \prod_i e^{-\Sigma_t^i t_i} \tag{2-37}$$

or as

$$\Phi_u = \Phi_0 \prod_i \frac{\Phi_i}{\Phi_0} , \tag{2-38}$$

where Φ_i is the uncollided flux at the point when only the ith shell is present. The quotient Φ_i/Φ_0 is the material attenuation factor for the ith zone. A relationship similar to Equation (2-38) can be assumed for the dose when several perturbations are introduced in the shield.

Thus, the dose can be approximated by

$$D = D_0 \prod_i \frac{D_i}{D_0} , \tag{2-39}$$

where D_i is the dose when only the ith zone in the shield is perturbed. Equation (2-39) can also be written as

$$D_0 + \Delta D - D_0 \prod_i \left(1 + \frac{\Delta D_i}{D_0}\right) \tag{2-40}$$

By expanding the product and ignoring the product of two incremental quantities, Equation (2-40) becomes

$$D_0 + \Delta D = D_0 \left(1 + \sum_i \frac{\Delta D_i}{D_0}\right). \tag{2-41}$$

Solving for the change in dose gives

$$\Delta D = \sum_i \Delta D_i, \tag{2-42}$$

which is the linear approximation. Thus, Equation (2-39) agrees with the linear approximation for small perturbations and is more accurate for larger perturbations. Also, Equation (2-39) never predicts a negative dose as long as all the D_i's are positive.

Substituting Equation (2-31) into Equation (2-40) yields

$$D = D_0 \prod_i \left[1 + \frac{\Delta \rho_i}{D_0 \rho_0} \int_{Z_i} \Phi^+(\bar{P})\, f_0(\bar{P})\, d\bar{P}\right]. \tag{2-43}$$

Substituting Equation (2-35) into Equation (2-43) yields

$$D = D_0 \prod_i \left\{ 1 + \frac{\Delta\rho_i}{D_0 \rho_0^i} \int_{\bar{Z}_i} \Phi_0^+(\bar{P})\, f_0(\bar{P}) \exp\left[-(r_b^i(\bar{P}) - r)\left(\frac{\rho_i}{\rho_0^i} - 1\right) \overline{\frac{\partial \ell n \Phi_0^+(\bar{P})}{\partial r}} \right] d\bar{P} \right\} . \tag{2-44}$$

Equation (2-44) can be written as

$$D = D_0 \prod_i \left\{ 1 + \frac{\alpha_i}{D_0} \int_{\bar{Z}_i} A(\bar{P}) \exp\left[-B(\bar{P})\, \alpha_i \right] d\bar{P} \right\} , \tag{2-45}$$

where

$$\alpha_i \equiv \frac{\Delta\rho_i}{\rho_0^i} ,$$

$$A(\bar{P}) \equiv \Phi_0^+(\bar{P})\, f_0(\bar{P}),$$

and $$B(\bar{P}) \equiv (r_b^i(\bar{P}) - r) \overline{\frac{\partial \ell n \Phi_0^+(\bar{P})}{\partial r}} .$$

Equation (2-45) is the desired expression for the dose as a function of changes in zone thickness in a one-dimensional shield. The approximations made in deriving Equation (2-45) are:

1. The changes in zone thicknesses can be approximated by a change in density of the zone.

2. The perturbed adjoint flux can be approximated by Equation (2-35).

3. The effect of several perturbations can be approximated by Equation (2-39).

Equation (2-45) can be used in conjunction with a function minimization algorithm to obtain an optimized shield. The only restriction is that the three approximations listed above do not substantially affect the final result. The results presented in Chapter IV were obtained using Equation (2-45).

In order to investigate the usefulness of Equation (2-45) for evaluating an initial configuration, the partial derivative of Equation (2-45) with respect to α_j is determined:

$$\frac{\partial D}{\partial \alpha_j} = \prod_{i \neq j} \left\{ 1 + \frac{\alpha_i}{D_0} \int_{\bar{Z}_i} A(\bar{P}) \exp\left[-B(\bar{P})\, \alpha_i\right] d\bar{P} \right\}$$

$$\cdot \left\{ \int_{\bar{Z}_j} A(\bar{P}) \left[1 - \alpha_j B(\bar{P})\right] \exp\left[-B(\bar{P})\, \alpha_j\right] d\bar{P} \right\} . \qquad (2\text{-}46)$$

Evaluating this expression for the initial configuration (all α_i equal to zero) yields

$$\frac{\partial D}{\partial \alpha_j}\Big|_0 = \int_{\bar{Z}_j} A(\bar{P})\, d\bar{P} \qquad (2\text{-}47)$$

$$= \int_{\bar{Z}_j} \Phi_0^+(\bar{P})\, f_0(\bar{P})\, d\bar{P} .$$

and

$$\frac{\partial D}{\partial \rho_j}\Big|_0 = \frac{\partial D}{\partial \alpha_j}\Big|_0 \frac{d\alpha_j}{d\rho_j} = \frac{1}{\rho_{j_0}} \int_{\bar{Z}_j} \Phi_0^+(\bar{P})\, f_0(\bar{P})\, d\bar{P} . \qquad (2\text{-}48)$$

Equation (2-48) is identical to Equation (2-32). Since only the density change approximation was used in deriving Equation (2-32), only this approximation introduces any errors in an optimized shield configuration obtained using Equation (2-46). The other two approximations only affect the rate of convergence of any iterative procedure which utilizes Equation (2-45) or Equation (2-46).

IV. THE OPTIMIZATION PROCEDURE

The optimization procedure to be used is based on the ASOP method described in Chapter I. In order to evaluate the constant terms appearing in Equations (1-7) through (1-11), it is necessary to define the vector $\bar{X}$ which describes the shield configuration. The rate of change of dose with respect to X_i can then be calculated using the chain rule:

$$\frac{\partial D}{\partial X_i} = \sum_{j=1}^{n} \frac{\partial D}{\partial \alpha_j} \frac{\partial \alpha_j}{\partial X_i}, \tag{2-49}$$

where $\frac{\partial D}{\partial \alpha_j}$ is given by Equation (2-46).

One possible choice is to define X_i to be the thickness of the ith zone. In this case, the zone thickness case, Equation (2-49) becomes

$$\frac{\partial D}{\partial X_i} = \frac{\partial D}{\partial \alpha_i} \frac{\partial \alpha_i}{\partial X_i}. \tag{2-50}$$

The alphas are related to the actual perturbed shield configuration by

$$\alpha_i = \frac{\rho_i - \rho_0^i}{\rho_0^i} = \frac{r_{i+1} - r_i}{r_0^{i+1} - r_0^i} - 1, \tag{2-51}$$

where the r's are the actual zone boundaries in the perturbed shield (no density approximation) and the r_0's are the zone boundaries in the unperturbed shield. Taking the partial derivative of Equation (2-51) with respect to X_i yields

$$\frac{\partial \alpha_i}{\partial X_i} = \frac{1}{r_0^{i+1} - r_0^i}. \tag{2-52}$$

Substituting Equation (2-52) into Equation (2-50) yields

$$\frac{\partial D}{\partial X_i} = \frac{1}{r_0^{i+1} - r_0^i} \frac{\partial D}{\partial \alpha_i}. \tag{2-53}$$

Another possibility is to define X_i to be r_i. In this case, Equation (2-49) becomes

$$\frac{\partial D}{\partial X_i} = \frac{\partial D}{\partial \alpha_{i-1}} \frac{\partial \alpha_{i-1}}{\partial X_i} + \frac{\partial D}{\partial \alpha_i} \frac{\partial \alpha_i}{\partial X_i}$$

or

$$\frac{\partial D}{\partial X_i} = \frac{1}{r_0^i - r_0^{i-1}} \frac{\partial D}{\partial \alpha_{i-1}} - \frac{1}{r_0^{i+1} - r_0^i} \frac{\partial D}{\partial \alpha_i}. \tag{2-54}$$

The second term in Equation (2-54) vanishes when X_i is the outside boundary of the system.

A more general way to define the X_i's is to let X_i be the amount that boundaries i through $i + k_i$ are moved, where k_i is the number of

succeeding boundaries to be moved simultaneously with boundary i. For example if k_i is zero, no boundaries are moved with boundary i, and X_i becomes r_i. Also, the special case in which k_i is chosen such that the ith boundary and all successive boundaries are moved simultaneously corresponds to the zone thickness definition. Using this more general definition, Equation (2-49) becomes

$$\frac{\partial D}{\partial X_i} = \frac{\partial D}{\partial \alpha_{i-1}} \frac{\partial \alpha_{i-1}}{\partial X_i} + \frac{\partial D}{\partial \alpha_{i+k_i}} \frac{\partial \alpha_{i+k_i}}{\partial X_i}$$

or

$$\frac{\partial D}{\partial X_i} = \frac{1}{r_0^i - r_0^{i-1}} \frac{\partial D}{\partial \alpha_{i-1}} - \frac{1}{r_0^{i+k_i+1} - r_0^{i+k_i}} \frac{\partial D}{\partial \alpha_{i+k_i}} . \qquad (2\text{-}55)$$

As before, the second term in Equation (2-55) vanishes when boundary $i + k_i$ is the outside boundary of the system.

Using the more general definition for X_i, the rate of change of the weight with respect to X_i is given by the chain rule as

$$\frac{\partial W}{\partial X_i} = \sum_{j=i}^{i+k_i} \frac{\partial W}{\partial r_j} \frac{\partial r_j}{\partial X_i}$$

or

$$\frac{\partial W}{\partial X_i} = \sum_{j=i}^{i+k_i} \frac{\partial W}{\partial r_j} . \qquad (2\text{-}56)$$

In one dimensional geometries,

$$\frac{\partial W}{\partial r_j} = (\rho_0^{j-1} - \rho_0^j) \cdot \begin{Bmatrix} 1 \text{ - slab} \\ 2\pi r \text{ - cylinder} \\ 4\pi r^2 \text{ - sphere} \end{Bmatrix} . \tag{2-57}$$

The ASOP method assumes the following expression for the dose

$$D = D_0 \exp[\sum_i A_i \delta X_i] . \tag{2-58}$$

Taking the partial derivative of Equation (2-58) with respect to X_i yields

$$\frac{\partial D}{\partial X_i} = A_i D_0 \exp[\sum_i A_i \delta X_i] . \tag{2-59}$$

Dividing Equation (2-59) by Equation (2-58) yields

$$A_i = [\frac{1}{D} \frac{\partial D}{\partial X_i}]_{X_i} , \tag{2-60}$$

where D and $\frac{\partial D}{\partial X_i}$ are obtained from Equations (2-45) and (2-55) respectively.

The dose-weight derivative can be evaluated using the relationship:

$$\frac{\partial D}{\partial W} = \frac{\partial D}{\partial X_i} \Big/ \frac{\partial W}{\partial X_i} , \tag{2-61}$$

where $\frac{\partial D}{\partial X_i}$ and $\frac{\partial W}{\partial X_i}$ are given by Equations (2-55) and (2-56) respectively.

The $[\frac{\partial}{\partial X_i}(\frac{\partial D}{\partial W})]$ terms in Equation (1-11) can be evaluated using a finite difference approximation of the form

$$[\frac{\partial}{\partial X_i}(\frac{\partial D}{\partial W})]_{X_i} = \frac{(\frac{\partial D}{\partial W})_{X_{i+\varepsilon}} - (\frac{\partial D}{\partial W})_{X_{i-\varepsilon}}}{2\varepsilon} \qquad (2\text{-}62)$$

where ε is a relatively small number.

In summary, the optimization procedure can be outlined as follows:

1. Evaluate $\Phi_0(\bar{P})$ and $\Phi_0^+(\bar{P})$. This requires two transport calculations.

2. Use the ASOP optimization procedure described in Chapter I to obtain a new estimate of the optimized configuration, but evaluate the constants in Equations (1-7) through (1-11) using Equations (2-60), (2-61), and (2-62).

3. Since Equations (2-60), (2-61), and (2-62) may not be accurate for large changes in the configuration, limit the amount the shield configuration is allowed to change to some arbitrary but reasonable value.

4. Repeat steps 1. through 3. until some convergence criteria on the dose and weight are met.

CHAPTER III

IMPLEMENTATION OF THE CALCULATIONAL METHOD

In this chapter, several concepts of importance to shielding calculations are discussed. Included are coupled neutron-gamma ray calculations and multigroup transport calculations. Also, the computer program used and the modifications made are described.

I. COUPLED NEUTRON-GAMMA RAY CALCULATIONS

Using the notation introduced in Chapter II, the Boltzmann equation for neutrons may be written as

$$\hat{H}\Phi_n(\bar{P}_n) = S_n(\bar{P}_n), \tag{3-1}$$

where the subscript n indicates neutron.

Similarly, the Boltzmann equation for gamma rays may be written as

$$\hat{H}\Phi_\gamma(\bar{P}_\gamma) = S_\gamma(\bar{P}_\gamma) + \int\int \Phi_n(\bar{P}_n)\, \Sigma_{n\gamma}(\bar{r}; E_n, \bar{\Omega}_n \rightarrow E_\gamma, \bar{\Omega}_\gamma)\, dE_n d\bar{\Omega}_n, \tag{3-2}$$

where $\Sigma_{n\gamma}(\bar{r}; E_n, \bar{\Omega}_n \rightarrow E_\gamma, \bar{\Omega}_\gamma)$ is the gamma-ray production cross section due to capture and inelastic scattering. Fission gammas are sometimes included in this cross section also. A term similar to the secondary gamma ray production term in Equation (3-2) could have been included in Equation (3-1) to account for photo-production of neutrons. However, since photoneutrons are seldom of importance in shielding calculations, they will be ignored.

The neutron and gamma ray doses may be defined by the following equations:

$$D_n = \int R_n(\bar{P}_n)\ \Phi_n(\bar{P}_n)\ d\bar{P}_n \tag{3-3}$$

and

$$D_\gamma = \int R_\gamma(\bar{P}_\gamma)\ \Phi_\gamma(\bar{P}_\gamma)\ d\bar{P}_\gamma, \tag{3-4}$$

where $R_n(\bar{P}_n)$ and $R_\gamma(\bar{P}_\gamma)$ are neutron and gamma ray response functions.

The adjoint concept may be introduced by making the following definitions:

$$\hat{H}^+\Phi^+_{n,n}(\bar{P}_n) \equiv R_n(\bar{P}_n) \tag{3-5}$$

and

$$\hat{H}^+\Phi^+_{\gamma,\gamma}(\bar{P}_\gamma) \equiv R_\gamma(\bar{P}_\gamma). \tag{3-6}$$

These definitions are consistent with the development in Chapter II. Thus, $\Phi^+_{n,n}(\bar{P}_n)$ is the probability that a neutron at position $\bar{P}_n$ will contribute to the neutron dose, and $\Phi^+_{\gamma,\gamma}(\bar{P}_\gamma)$ is the probability that a gamma ray at position $\bar{P}_\gamma$ will contribute to gamma dose.

The gamma ray source resulting from neutron interactions is given by the secondary production term in Equation (3-2). The contribution of this source to the gamma ray dose is given by the following expression:

$$D_{n,\gamma} = \iiint \Phi^+_{\gamma,\gamma}(\bar{r},E_\gamma,\bar{\Omega}_\gamma)\ \left[\iint \Phi_n(\bar{r},E_n,\bar{\Omega}_n)\Sigma_{n\gamma}(\bar{r};E_n,\bar{\Omega}_n\rightarrow E_\gamma,\bar{\Omega}_\gamma)dE_n d\bar{\Omega}_n\right]d\bar{r}dE_\gamma d\bar{\Omega}_\gamma. \tag{3-7}$$

Equation (3-7) may be written as

$$D_{n,\gamma} = \int R_{n,\gamma}(\bar{P}_n)\ \Phi_n(\bar{P}_n)\ d\bar{P}_n, \tag{3-8}$$

where

$$R_{n,\gamma}(\bar{P}_n) \equiv \iint \Phi^+_{\gamma,\gamma}(\bar{r},E_\gamma,\bar{\Omega}_\gamma)\ \Sigma_{n\gamma}(\bar{r};E_n,\bar{\Omega}_n\rightarrow E_\gamma,\bar{\Omega}_\gamma)\ dE_\gamma d\bar{\Omega}_\gamma. \tag{3-9}$$

Then the following definition may be made:

$$\hat{H}^+\Phi^+_{n,\gamma}(\bar{P}) = R_{n,\gamma}(\bar{P}_n). \tag{3-10}$$

Substituting Equation (3-6) into Equation (3-4) yields:

$$D_\gamma = \int \Phi_\gamma(\bar{P}_\gamma)\ H^+\Phi^+_{\gamma,\gamma}(\bar{P}_\gamma)\ d\bar{P}_\gamma. \tag{3-11}$$

Using the definition of the adjoint operator, Equation (2-10), with the boundary term made zero by the boundary conditions, Equation (3-11) becomes

$$D_\gamma = \int \Phi^+_{\gamma,\gamma}(\bar{P}_\gamma)\ \hat{H}\Phi_\gamma(\bar{P}_\gamma)\ d\bar{P}_\gamma. \tag{3-12}$$

Substituting Equation (3-2) into Equation (3-12) yields:

$$D_\gamma = \int \Phi^{-1}_{\gamma,\gamma}(\bar{P}_\gamma)\ S_\gamma(\bar{P}_\gamma)\ d\bar{P}_\gamma$$

$$+ \iiint \Phi^+_{\gamma,\gamma}(\bar{r},E,\bar{\Omega}_\gamma)\Big[\iint \Phi_n(r,E_n,\bar{\Omega}_n)\ \Sigma_{n\gamma}(\bar{r};E_n,\bar{\Omega}_n\rightarrow E_\gamma,\bar{\Omega}_\gamma)\ dE_n d\bar{\Omega}_n\Big] d\bar{r} dE_\gamma d\bar{\Omega}_\gamma. \tag{3-13}$$

Using Equations (3-7) and (3-8), Equation (3-13) becomes

$$D_\gamma = \int \Phi^+_{\gamma,\gamma}(\bar{P}_\gamma)\ S_\gamma(\bar{P}_\gamma)\ d\bar{P}_\gamma + D_{n,\gamma} \tag{3-14}$$

or

$$D_\gamma = \int \Phi^+_{\gamma,\gamma}(\bar{P}_\gamma)\, S_\gamma(\bar{P}_\gamma)\, d\bar{P}_\gamma + \int \Phi_n(\bar{P}_n)\, R_{n,\gamma}(\bar{P}_n)\, d\bar{P}_n. \tag{3-15}$$

Substituting Equation (3-10) into Equation (3-15) yields

$$D_\gamma = \int \Phi^+_{\gamma,\gamma}(\bar{P}_\gamma)\, S_\gamma(\bar{P}_\gamma)\, d\bar{P}_\gamma + \int \Phi_n(P_n)\, \hat{H}^+ \Phi^+_{n,\gamma}(\bar{P}_n)\, d\bar{P}_n. \tag{3-16}$$

Using the definition of the adjoint operator, Equation (3-16) becomes

$$D_\gamma = \int \Phi^+_{\gamma,\gamma}(\bar{P}_\gamma)\, S_\gamma(\bar{P}_\gamma)\, d\bar{P}_\gamma + \int \Phi^+_{n,\gamma}(\bar{P}_n)\, \hat{H}\Phi_n(\bar{P}_n)\, d\bar{P}_n. \tag{3-17}$$

Substituting Equation (3-1) into Equation(3-17) yields

$$D_\gamma = \int \Phi^+_{\gamma,\gamma}(\bar{P}_\gamma)\, S_\gamma(\bar{P}_\gamma)\, d\bar{P}_\gamma + \int \Phi^+_{n,\gamma}(\bar{P}_n)\, S_n(\bar{P}_n)\, d\bar{P}_n. \tag{3-18}$$

Equation (2-19) may be written as

$$D_n = \int \Phi_n(\bar{P}_n)\, R_n(\bar{P}_n)\, d\bar{P}_n = \int \Phi^+_{n,n}(\bar{P}_n)\, S(\bar{P}_n)\, d\bar{P}_n. \tag{3-19}$$

Combining Equations (3-4) and (3-18) yields

$$D_\gamma = \int \Phi_\gamma(\bar{P}_\gamma)\, R_\gamma(\bar{P}_\gamma)\, d\bar{P}_\gamma = \int \Phi^+_{\gamma,\gamma}(\bar{P}\gamma)\, S_\gamma(\bar{P}_\gamma)\, d\bar{P}_\gamma + \int \Phi^!_{n,\gamma}(\bar{P}_n)\, S_n(\bar{P}_n)\, d\bar{P}_n. \tag{3-20}$$

Adding Equations (3-19) and (3-20) yields

$$\begin{aligned} D &= \int \Phi_n(\bar{F}_n)\, R_n(\bar{\Gamma}_n)\, d\bar{P}_n + \int \Phi_\gamma(\bar{F}_\gamma)\, R_\gamma(\bar{\Gamma}_\gamma)\, d\bar{P}_\gamma \\ &= \int [\Phi^+_{n,n}(\bar{P}_n) + \Phi^+_{n,\gamma}(\bar{P}_n)]\, S_n(\bar{P}_n)\, d\bar{P}_n + \int \Phi^+_{\gamma,\gamma}(\bar{P}_\gamma)\, S_\gamma(\bar{P}_\gamma)\, d\bar{P}_\gamma. \end{aligned} \tag{3-21}$$

Note in Equation (3-21) that both $\Phi^{+}_{n,n}(\bar{P}_n)$ and $\Phi^{+}_{n,\gamma}(\bar{P}_n)$ need not be calculated but only their sum. Thus, Equation (3-2) may be written as

$$D = \int \Phi^{+}_{n,D}(\bar{P}_n)\, S_n(\bar{P}_n)\, d\bar{P}_n + \int \Phi^{+}_{\gamma,\gamma}(\bar{P}_\gamma)\, S_\gamma(\bar{P}_\gamma)\, d\bar{P}_\gamma, \tag{3-22}$$

where

$$\Phi^{+}_{n,D}(\bar{P}_n) \equiv \Phi^{+}_{n,n}(\bar{P}_n) + \Phi^{+}_{n,\gamma}(\bar{P}_n).$$

Adding Equations (3-5) and (3-10) yields

$$\hat{H}^{+}\Phi^{+}_{n,n}(\bar{P}_n) + \hat{H}^{+}\Phi^{+}_{n,\gamma}(\bar{P}_n) = R_n(\bar{P}_n) + R_{n,\gamma}(\bar{P}_n)$$

or

$$\hat{H}^{+}\Phi^{+}_{n,D}(\bar{P}_n) = R_n(\bar{P}_n) + R_{n,\gamma}(\bar{P}_n). \tag{3-23}$$

The above development is a generalization of the concept of neutron importance for coupled neutron-gamma ray transport calculations. Equations (3-1) and (3-2) can be solved to obtain the neutron and gamma ray fluxes. Note that the neutron flux does not depend upon the gamma ray flux, while the gamma ray flux is coupled to the neutron flux by the secondary gamma ray production term in Equation (3-2). Equations (3-6) and (3-23) can be solved to obtain adjoint neutron and gamma ray fluxes. Note that the adjoint gamma ray flux does not depend upon the adjoint neutron flux, while the adjoint neutron flux is coupled to the adjoint gamma ray flux by the $R_{n,\gamma}(\bar{P}_n)$ term in Equation (3-23) which is given by Equation (3-9). It can be seen from Equation (3-22) that

$\Phi^{+}_{n,D}(\bar{P}_n)$ is the probability that a neutron at $\bar{P}_n$ will contribute to the dose and that $\Phi^{+}_{\gamma,\gamma}(\bar{P}_\gamma)$ is the probability that a gamma ray at $\bar{P}_\gamma$ will contribute to the dose. Equation (3-22) can be considered a generalization of Equation (2-19) for the coupled problem.

II. MULTIGROUP TRANSPORT CALCULATIONS

The multigroup form of the Boltzmann equation can be obtained by integrating each term of Equation (2-1) over the energy interval ΔE_g. The result is (18)

$$\nabla\cdot\bar{\Omega}\Phi_g(\bar{r},\bar{\Omega}) + \Sigma_t^g(\bar{r})\ \Phi_g(\bar{r},\bar{\Omega}) = S_g(\bar{r},\bar{\Omega}) + \sum_{g'=1}^{G}\int\Sigma_s^{g'\to g}(\bar{r},\bar{\Omega}'\to\bar{\Omega})\ \Phi_{g'}(\bar{r},\bar{\Omega}')\ d\bar{\Omega}', \qquad (3\text{-}24)$$

where G is the number of groups.

The coupled neutron-gamma ray transport problem described by Equations (3-1) and (3-2) can be combined into one calculation by including the gamma ray groups as additional groups below the neutron groups. The secondary gamma ray production term represents a group to group transfer just as the scattering term in a neutron or gamma ray transport problem does. Thus the procedure for solving a coupled transport problem can be the same as the procedure used to solve one particle transport problems.

The multigroup form of the equation adjoint to the Boltzmann equation is (18)

$$-\nabla\cdot\bar{\Omega}\Phi_g^+(\bar{r},\bar{\Omega}) + \Sigma_t^g(\bar{r})\ \Phi_g^+(\bar{r},\bar{\Omega}) = R_g(\bar{r},\bar{\Omega})$$

$$+\sum_{g'=1}^{G}\int\Sigma_s^{g\to g'}(\bar{r},\bar{\Omega}\to\bar{\Omega}')\ \Phi_g^+(\bar{r},\bar{\Omega}')\ d\bar{\Omega}', \qquad (3\text{-}25)$$

where the group averaged parameters may be defined in more than one way (18).

The adjoint, coupled neutron-gamma ray transport problem described by Equations (3-6) and (3-23) can also be combined into one calculation by including the gamma ray groups as additional groups below the neutron groups. The $R_{n,\gamma}(\bar{P}_n)$ in Equation (3-23) is given by Equation (3-9) and has the same form as the scattering term in Equation (2-11). Thus Equations (3-24) and (3-25) can represent a neutron problem, a gamma ray problem, or a coupled neutron-gamma ray problem.

Equation (3-24) can be written as

$$\hat{H}_g\Phi_g(\bar{P}) = S_g(\bar{P}), \qquad (3\text{-}26)$$

where $\bar{P}$ now represents position and direction but not energy phase space.

Equation (3-26) is the multigroup form of Equation (2-2). The group form of the difference flux formulations is

$$\Phi_g(\bar{P}) = \Phi_g^o(\bar{P}) + \delta\Phi_g(\bar{P}), \qquad (3\text{-}27)$$

where $\delta\Phi_g(\bar{P})$ is the group averaged difference flux.

The group form of Equation (2-8) is

$$\hat{H}_g \delta\Phi_g(\bar{P}) = f_g(\bar{P}), \tag{3-28}$$

where

$$f_g(\bar{P}) = [\hat{H}_g^0 - \hat{H}_g]\ \Phi_g^0(\bar{P}). \tag{3-29}$$

When group g is a gamma ray group in a coupled neutron-gamma ray problem, the "scattering" term in the equivalent source (see Equation (2-25)) includes neutron to gamma ray transitions as well as the true scattering term.

III. COMPUTER PROGRAM MODIFICATIONS

The coupled neutron-gamma ray transport calculations, Equations (3-24) and (3-25), were performed using the discrete ordinate method. A computer program was written to perform the following calculations as one automated calculation:

1. Perform the forward calculation represented by Equation (3-24) using ANISN (10) to obtain $\Phi_g^0(\bar{P})$.

2. Calculate $f_g^0(\bar{P})$ (see Equation (2-28)) using the equation

$$f_g^0(\bar{r},\bar{\Omega}) = \sum_{g'=1}^{G} \int \Sigma_{s0}^{g'\to g}(\bar{r},\bar{\Omega}'\to\bar{\Omega})\ \Phi_{g'}^0(\bar{r},\bar{\Omega}')\ d\bar{\Omega}' - \Sigma_{t0}^{g}(\bar{r})\ \Phi_g^0 . \tag{3-30}$$

The first term in Equation (3-30) is the scattering source in Equation (3-24) and is available from the calculation of $\Phi_g^0(\bar{P})$.

3. Calculate D_0 using Equation (2-22).

4. Perform the adjoint calculation represented by Equation (3-25) to obtain $\Phi^{+}_{gO}(\bar{P})$.

5. Calculate the quantity $\overline{\frac{\partial \ell n \Phi^{+}_{gO}(\bar{P})}{\partial r}}$ for each zone, energy group, and discrete ordinate in the quadrature. This slope is calculated using two space points near the center of the zone.

6. Use the optimization procedure described in Chapter II to obtain a new shield configuration.

7. Modify the ANISN space mesh and zone map to describe the new shield configuration.

8. Repeat steps one through seven until some convergence criteria are met.

Equations (2-43) and (2-46) require integrations over all phase space. ANISN performs integrations of this type by using energy groups to describe energy dependence, a space mesh to describe spatial dependence, and an angular mesh characterized by discrete values of the angular coordinates to describe angular dependence. The integration over all phase space is evaluated using

$$\iiint X(\bar{r},E,\bar{\Omega})\, d\bar{r}dEd\bar{\Omega} \cong \sum_{g=1}^{IGM} \sum_{I=1}^{IM} \sum_{D=1}^{MM} X_{D,I,g} W_D V_I, \qquad (3\text{-}31)$$

where

$X(\bar{r},E,\bar{\Omega})$ is any arbitrary function,

IGM is the total number of energy groups (neutron plus gamma),

IM is the number of intervals in the space mesh,

MM is the number of discrete angles in the quadrature formula,

$X_{D,I,G}$ the average values of $X_G(\bar{r},\bar{\Omega})$ in space mesh I and angular mesh D,

$X_G(r,\bar{\Omega})$ is the integral of $X(\bar{r},E,\bar{\Omega})$ over energy group G,

W_D is the quadrature weight of angle D,

and V_I is the volume of mesh interval I.

This same method was used when either Equation (2-43) or Equation (2-46) was evaluated in step six above.

CHAPTER IV

PRESENTATION OF RESULTS

When possible, it is desirable to compare the results of a new computational procedure with the results obtained from an independent calculation in which one has confidence. Ideally the two calculations would be completely uncorrelated. Then good agreement would lend confidence to the answers obtained. Unfortunately, it would probably not be possible to reproduce most published shield optimization results, and it would be difficult or impossible to determine what caused the discrepancies. For this reason, the sample ASOP problem (8) was chosen for a test problem. Since both ASOP and the calculations performed here use ANISN, there should be no large discrepancies caused by differences in the transport calculations. Also, using exactly the same cross sections eliminates another possible source of disagreement.

The sample ASOP problem consists of a spherical model of a SNAP-8 ZrH reference reactor and a shield. The shield contains four layers as shown in Figure 1. The compositions of the shielding materials are given in Table 1. The LiH-stainless steel has a density of 1.026 grams per cubic centimeter, and the tungsten has a density of 18.61 grams per cubic centimeter. The reactor model contains a reactor core, grid, plenum, and vessel. The ANISN calculations were made using a 39 group cross section set containing 21 neutron groups and 18 gamma ray groups, an S_8 angular quadrature, 130 spatial intervals,

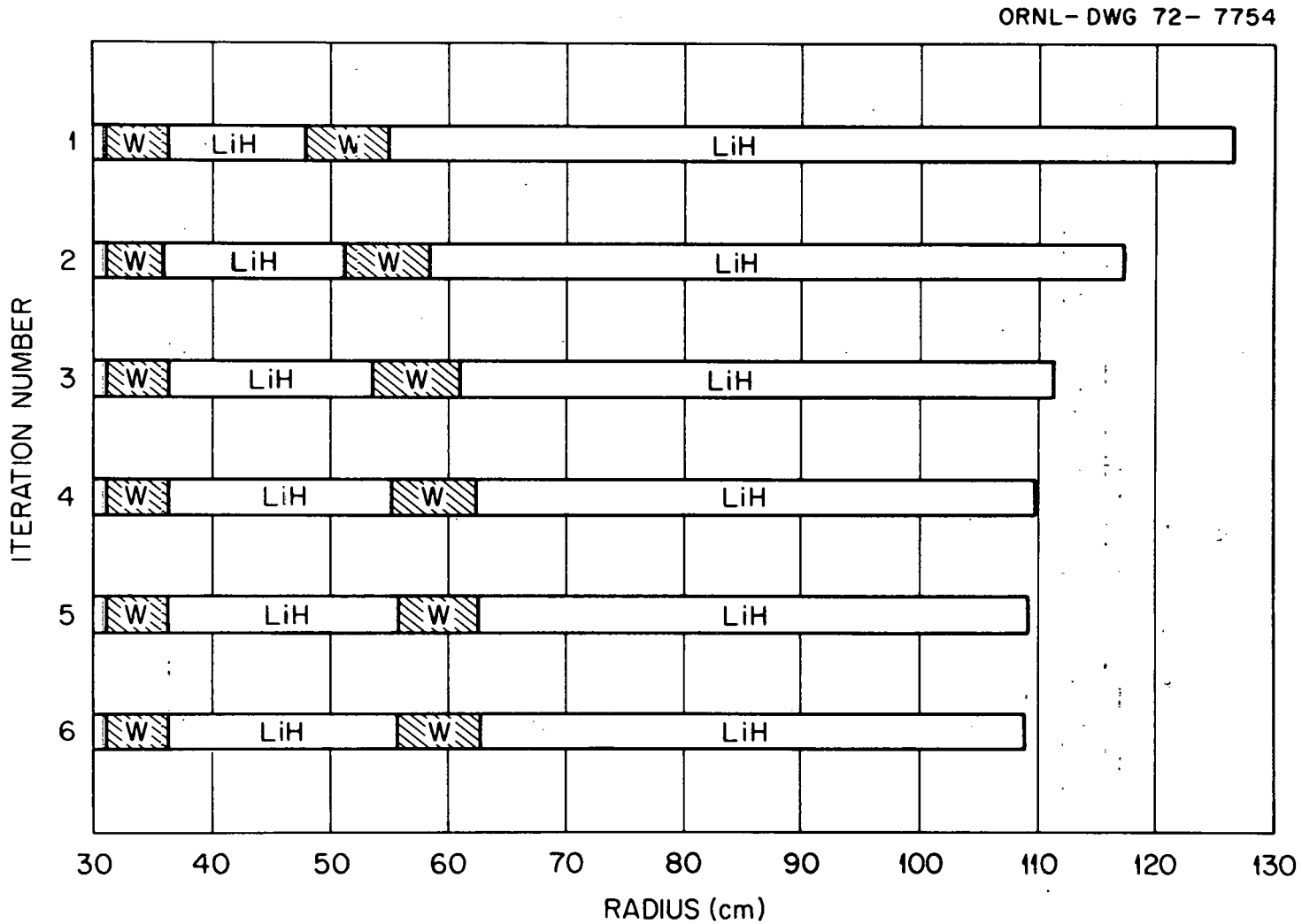

Figure 1. ASOP convergence of the sample ASOP problem.

TABLE 1

COMPOSITION OF PRINCIPAL SHIELD MATERIALS

Material	Density (atoms/barn-cm)
LiH-SS	
^{6}Li	0.0041188
^{7}Li	0.0506526
H	0.0547717
Fe	0.002068
Cr	0.0006274
Ni	0.0003816
Mo	0.0001111
W-Mo	
W	0.05972
Mo	0.002335
B_4C	
B	0.1108
C	0.0277

and an P_3 expansion of the transfer cross sections. The energy group structure and response functions are given in Table 2. The calculations are fixed source problems with a flat, fission spectrum source in the core normalized to a power of 600 kilowatts thermal. The dose constraint is that the dose rate at 3048 centimeters (100 feet) from the core center be 60 mrem per hour.

Figure 1 describes graphically the results of the ASOP calculation for the sample ASOP problem. Figure 2 shows similar results obtained using the methods developed in Chapter II. The computer program implementing these methods is named SHAPE, and this name will be used to identify the method. Comparison of Figure 1 and Figure 2 show that the convergence of the SHAPE calculation is very similar to the convergence of the ASOP calculation. It should be noted that nine ANISN calculations were required per iteration in the ASOP calculation, while only two ANISN calculations were required per iteration in the SHAPE calculation. Since the transport calculations dominate the computational effort in both methods, the number of ANISN calculations may be used as a measure of the efficiency of each method.

The weight, dose and the ratio of the maximum to minimum dose-weight derivatives obtained using ASOP and SHAPE are shown in Table 3. The dose for the initial configuration is slightly different in the two calculations because the SHAPE calculation used equal sized intervals in each zone for the first iteration, while the ASOP calculation used smaller intervals near zone boundaries. SHAPE used smaller intervals near zone boundaries for all iterations except the first iteration. The dose-weight derivative ratio is different for the two

TABLE 2

ENERGY GROUP STRUCTURE AND FLUENCE-TO-DOSE CONVERSION FACTORS

Group	Upper Energy (eV)	Fluence-to-Dose Conversion Factors (mrem/hr)/(part/cm^2/sec)
Neutrons:		
1	1.4918(+7)*	1.5000(-1)
2	1.0000(+7)	1.5000(-1)
3	6.7032(+6)	1.3700(-1)
4	4.4933(+6)	1.3200(-1)
5	3.0119(+6)	1.3100(-1)
6	2.0190(+6)	1.2500(-1)
7	1.3534(+6)	1.1600(-1)
8	9.0718(+5)	1.0600(-1)
9	5.5023(+5)	7.5700(-2)
10	3.3373(+5)	5.5100(-2)
11	2.0242(+5)	4.0100(-2)
12	1.2277(+5)	2.4500(-2)
13	4.0867(+4)	8.5000(-3)
14	1.1709(+4)	5.0000(-3)
15	3.3546(+3)	5.0000(-3)
16	7.4852(+2)	5.0000(-3)
17	1.6702(+2)	5.0000(-3)
18	3.7266(+1)	5.0000(-3)
19	8.3153(0)	5.0000(-3)
20	1.8554(0)	5.0000(-3)
21	4.1399(-1)	3.7500(-3)
Gamma Rays:		
22	1.0000(+7)	9.8000(-3)
23	8.0000(+6)	8.5000(-3)
24	7.0000(+6)	7.6000(-3)
25	6.0000(+6)	6.7000(-3)
26	5.0000(+6)	5.8000(-3)
27	4.0000(+6)	5.0000(-3)
28	3.5000(+6)	4.5000(-3)
29	3.0000(+6)	4.0000(-3)
30	2.5000(+6)	3.5000(-3)
31	2.0000(+6)	3.0000(-3)
32	1.6000(+6)	2.4000(-3)
33	1.2000(+6)	2.0000(-3)
34	9.0000(+5)	1.5000(-3)
35	6.0000(+5)	1.0500(-3)
36	4.0000(+5)	6.0000(-4)
37	2.1000(+5)	2.8000(-4)
38	1.2000(+5)	1.4000(-4)
39	7.0000(+4)	4.0000(-4)

*Read as 1.4918×10^7.

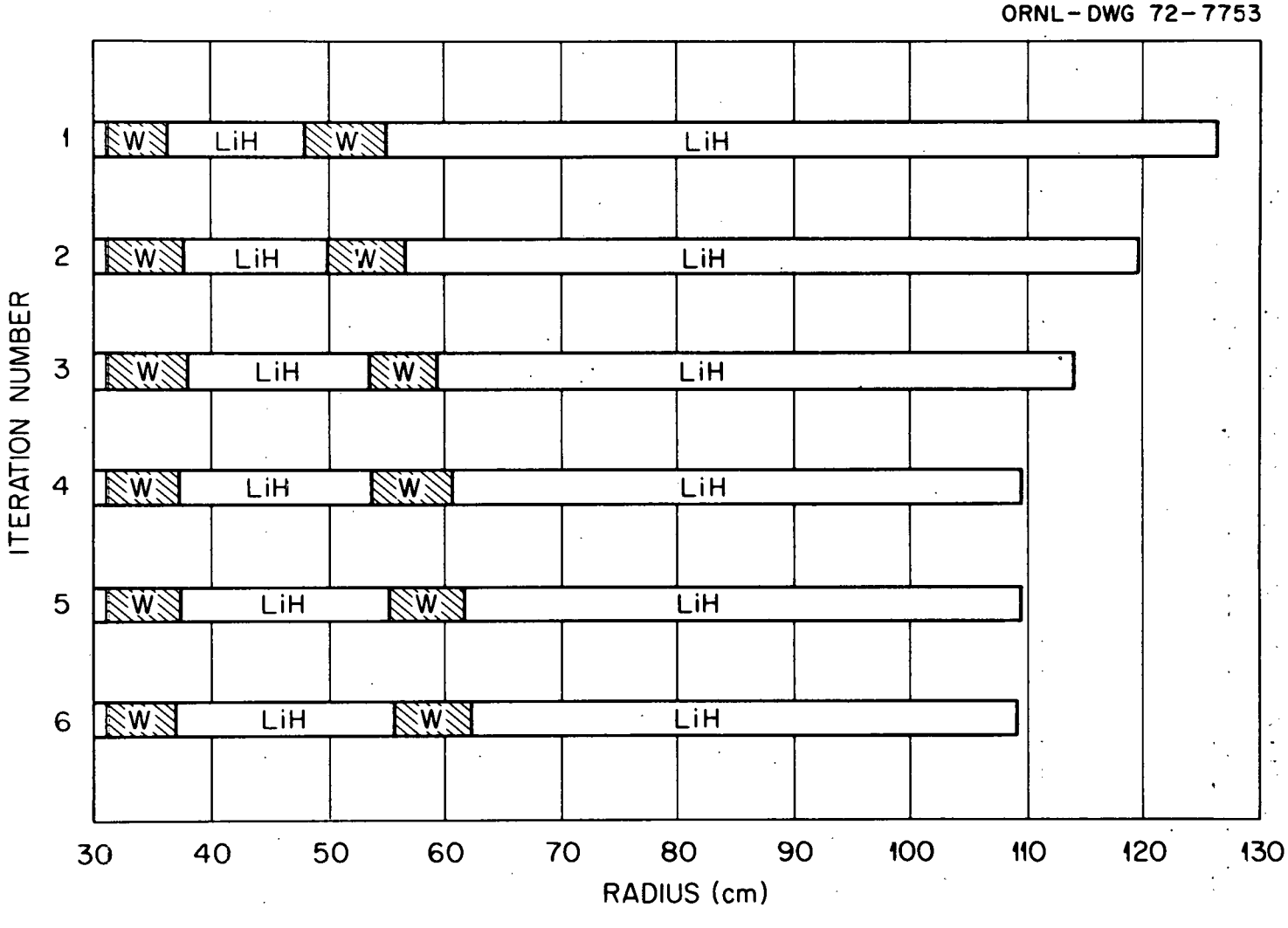

Figure 2. SHAPE convergence of the sample ASOP problem.

TABLE 3

COMPARISON OF THE CONVERGENCE OF ASOP AND SHAPE

ASOP

Iteration Number	Weight (Grams)	Dose (mrem/hr)	$\frac{\partial D}{\partial W}$ Maximum/Minimum
1.	1.400×10^7	62.54	5.61
2.	1.284×10^7	57.57	2.87
3.	1.245×10^7	55.60	1.61
4.	1.225×10^7	57.42	1.18
5.	1.216×10^7	59.22	1.04
6.	1.213×10^7	59.80	1.01
Projection	1.212×10^7	60.00	1.00

SHAPE

Iteration Number	Weight (Grams)	Dose (mrem/hr)	$\frac{\partial D}{\partial W}$ Maximum/Minimum
1.	1.400×10^7	63.76	3.03
2.	1.310×10^7	63.49	2.57
3.	1.205×10^7	71.45	1.88
4.	1.200×10^7	64.99	1.30
5.	1.201×10^7	63.41	1.19
6.	1.208×10^7	61.37	1.12
7.	1.211×10^7	60.66	1.08
8.	1.212×10^7	60.29	1.05
Projection	1.213×10^7	60.00	1.00

calculations because ASOP used a zone boundary movement definition for the dose-weight derivatives with the outside boundary of the second tungsten layer moved simultaneously with its inside boundary, while the SHAPE calculation used a zone thickness definition for the dose-weight derivative. Convergence criteria were that the dose be within one percent of the dose constraint and that the dose-weight derivative ratio be less than 1.15. The most important result to consider is the weight of the shield. Table 3 shows that the weights calculated by the two methods differ by one digit in the fourth significant figure. This agreement is more than adequate for most, if not all, engineering purposes. This agreement also tends to show that the SHAPE computer program contains no significant programing errors and that the equivalent density approximation does not significantly affect the shield weight, at least for shields similar to the one considered.

The converged shield dimensions and shield thicknesses for the sample ASOP problem are shown in Table 4. None of the boundary positions or zone thicknesses differ by much more than half a centimeter. While these parameters are more sensitive to the method used than the weight, the differences are probably not of practical importance. The fact that the first tungsten layer's thickness can change 11% without affecting the weight indicates that this thickness could be set at some non-optimum thickness in order to meet some other constraint such as maximum allowable heating without materially affecting the weight.

Two additional shielding problems were selected to further test the computational procedures and to demonstrate their versatility. The

TABLE 4

CONVERGED CONFIGURATION FOR THE SAMPLE ASOP PROBLEM

ASOP

Physical Region	Type	Outer Radius in cm	Thickness in cm
1	Core	18.89	
2	Grid	21.93	
3	Plenum	30.60	
4	Vessel	31.08	
5	W	36.29	5.21
6	LiH	55.88	19.59
7	W	62.79	6.91
8	LiH	109.01	46.22

SHAPE

Physical Region	Type	Outer Radius in cm	Thickness in cm
1	Core	18.89	
2	Grid	21.93	
3	Plenum	30.60	
4	Vessel	31.08	
5	W	36.87	5.79
6	LiH	56.36	19.49
7	W	63.03	6.67
8	LiH	108.64	45.61

second problem considered was the sample ASOP problem modified by the addition of two more shield layers as shown in Figure 3. The third problem considered was obtained by sandwiching each tungsten layer with layers of B_4C of density 2.54 grams per cubic centimeter. The optimized shield configurations obtained are shown in Figure 3. The zone boundaries and the zone thicknesses are given in Table 5. The six layer shield weighed 1.133×10^7 grams or 7% less than the four layer shield. The twelve layer shield weighed 1.104×10^7 grams or 3% less than the six layer shield. The percent weight decreases would be larger if the dose constraint had been lower or the reactor power higher. These two problems demonstrate that increasing the number of layers does not present any particular calculational difficulties. The convergence of these two problems was not significantly different than the convergence of the four layer problem. The third problem demonstrates the usefulness of this method for studying the effectiveness of different shielding materials in a particular shielding application. It should be noted that only two ANISN calculations per iteration were required for these problems, while ASOP would require thirteen and twenty five ANISN calculations per iteration for the same two problems.

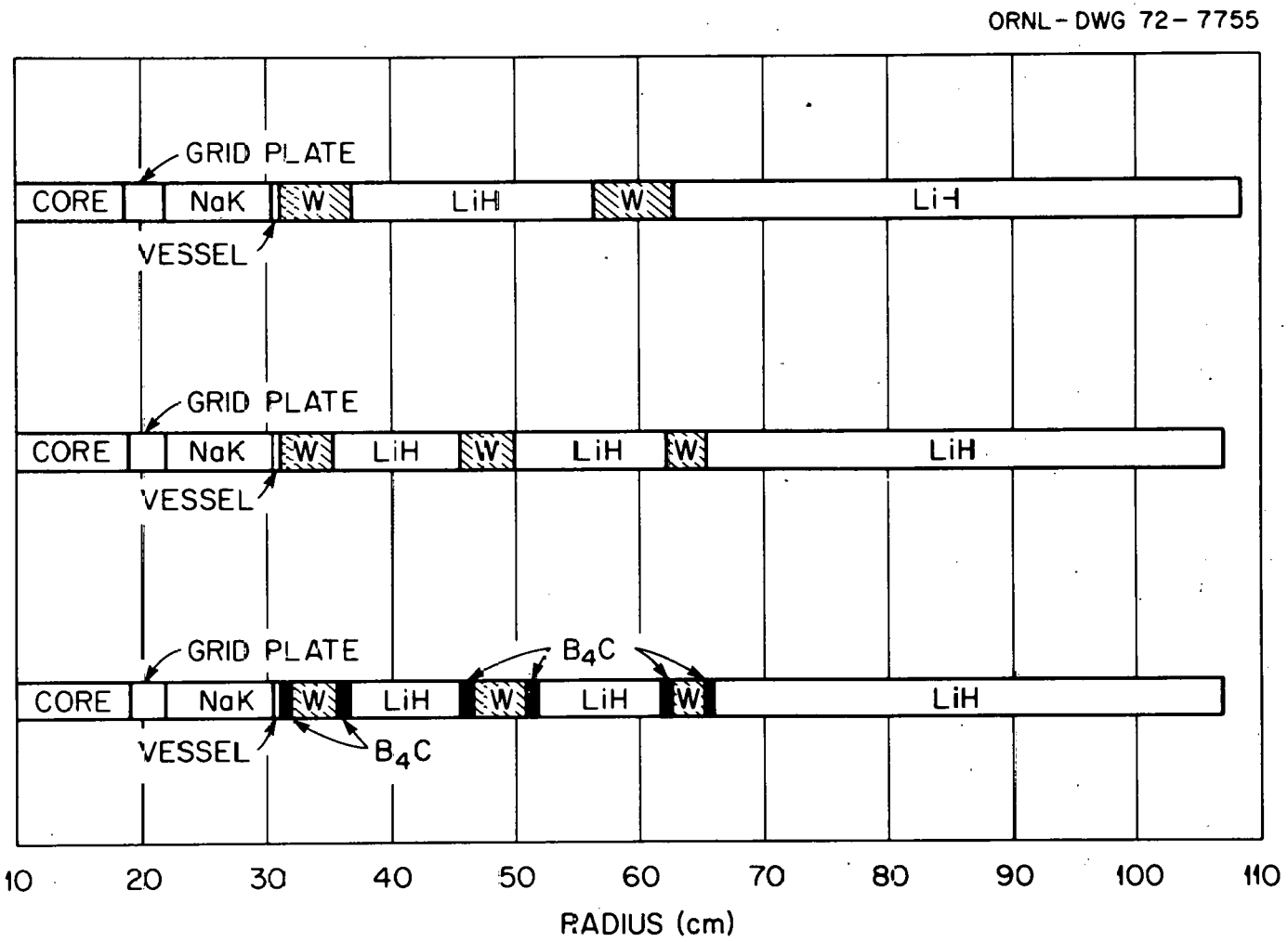

Figure 3. The three optimized shields.

TABLE 5

OPTIMIZED SHIELDS FOR PROBLEMS TWO AND THREE

Problem 2

Physical Region	Type	Outer Radius in cm	Thickness in cm
1	Core	18.89	
2	Grid	21.93	
3	Plenum	30.60	
4	Vessel	31.08	
5	W	35.23	4.15
6	LiH	45.58	10.35
7	W	50.06	4.48
8	LiH	62.28	12.22
9	W	65.50	3.22
10	LiH	106.97	41.47

Problem 3

Physical Region	Type	Outer Radius in cm	Thickness in cm
1	Core	18.89	
2	Grid	21.93	
3	Plenum	30.60	
4	Vessel	31.08	
5	B_4C	32.00	0.92
6	W	35.76	3.76
7	B_4C	36.67	0.91
8	LiH	45.39	8.72
9	B_4C	46.35	0.96
10	W	50.84	4.49
11	B_4C	51.72	0.88
12	LiH	61.64	9.91
13	B_4C	62.48	0.85
14	W	65.12	2.64
15	B_4C	65.73	0.61
16	LiH	106.97	41.24

CHAPTER V

SUMMARY

A method has been developed for the weight optimization of one-dimensional layered shields. The method is based on discrete ordinates transport calculations which allows the use of the best available cross section information through coupled neutron-gamma ray cross section sets. Results obtained using this method were compared with results from the computer program ASOP. The optimum weights calculated by the two methods for a representative SNAP reactor shield differed by approximately 0.1%. This agreement is considered to be satisfactory. The method also proved to require significantly less computer time than the ASOP program. This reduction in computer time was obtained using adjoint transport theory which proved to be a very effective way to obtain the information required for the shield optimization calculations. For the four layer SNAP shield, the new method was roughly a factor of three faster than the ASOP method. However, the time required for the ASOP method is approximately proportional to the number of design variables, while the time required for the new method is relatively independent of the number of design variables. For a twelve layer shield, the new method would be something like a factor of ten faster. A six layer and a twelve layer shield were optimized, and the results demonstrated that increasing the number of layers presented no particular problems.

It is felt that the results of this work are adequate for the practical design of one dimensional layered shields. A generalization of this problem is to allow the composition of the zones to vary as well

as the zone thicknesses. Several of the techniques used in this work are applicable to the generalized problem.

While the one-dimensional shield weight optimization problem has been investigated by a number of workers, very little work has been done on two-dimensional shield weight optimization. Many additional difficulties are encountered when a truly two-dimensional model is used instead of a one-dimensional model. The adjoint difference method could be used in two dimensions to evaluate the effect of moving a portion of a shield boundary a small amount. The equivalent density change approximation could be used in performing a calculation of this type.

THIS PAGE

WAS INTENTIONALLY

LEFT BLANK

BIBLIOGRAPHY

1. Bernick, R. L., "Application of the Method of Steepest Descent to Laminated Shield Weight Optimization," Rep. NAA-SR-Memo-8181, North American Aviation, Inc. (1963).

2. Bernick, R. L., "The OPEX Shield Optimization Code," Rep. NAA-SR-Memo-11516, North American Aviation, Inc. (1965).

3. Lahti, Gerald P., "OPEX-II, A Radiation Shield Optimization Code," NASA TMX-1769 (1969).

4. Lahti, Gerald P., "Application of the Method of Steepest Descent to Laminated Shield Weight Optimization with Several Constraints-Theory," NASA TMX-2435 (1971).

5. Clark, F. H. S. and F. B. K. Kam, "A Generalized One Constraint Lagrange Multiplier Numerical Formulation," ORNL-3742 (1965).

6. Troubetzkoy, E. S. and M. L. Wohl, "Unamit - A One-Dimensional 4π Spherical Multilayer Reactor-Shield-Weight Optimization Code," NASA TMX-2048 (1970).

7. Mynatt, F. R. et al., "Neutron Physics Division Annual Progress Report," ORNL-4134 (1967).

8. Engle, W. W., Jr. and F. R. Mynatt, "A Shield Optimization Technique with Direct Utilization of Transport Calculations," Trans. ANS, Vol. 12, No. 2 (1969).

9. Engle. W. W., Jr., "A User's Manual for ASOP, ANISN Shield Optimization Program," Union Carbide Corp., Nuclear Division, CTC-INF-941 (1969).

10. Engle, W. W., Jr., "A User's Manual for ANISN, A One-Dimensional Discrete Ordinates Transport Code with Anisotropic Scattering," USAEC Report K-1693 (1967).

11. Dalton, G. R. and R. K. Osborne, "Flux Perturbations by Thermal Neutron Detectors," Nuc. Sci. Engr. 9: 198-210 (1961).

12. Brandon, R. W., J. C. Robinson, and C. W. Craven, Jr., "A Variational Approach for the Determination of Neutron Flux Spectra from Detector Activation," Nuc. Sci. Engr. 39: 2, 151-163 (1970).

13. Lichtenstein, H., "Effects of Spatial Perturbations on Particle Transport in Otherwise Homogeneous Media," Unpublished Ph.D. Dissertation, New York City: Columbia University (1970).

14. Hoffman, T. J., J. C. Robinson, and P. N. Stevens, "The Adjoint Difference Method and its Application to Deep-Penetration Radiation Transport," Nuc. Sci. Engr. 48: 2, 179-188 (1972).

15. Weinberg, A. M. and E. P. Wigner, The Physical Theory of Neutron Chain Reactors, Chicago: University of Chicago Press (1958).

16. Bell, G. I. and S. Glasstone, Nuclear Reactor Theory, New York City: Van Nostrand Reinhold Company (1970).

17. Burgart, C. E., "06R-D, A Discrete Scattering Version of 06R with Importance Sampling of the Angle of Scatter," USAEC Report ORNL-TM-3031 (1970).

18. Straker, E. A., P. N. Stevens, D. C. Irving, and V. R. Cain, "The Monte Carlo Code - A Multigroup Neutron and Gamma-Ray Monte Carlo Transport Code," ORNL-4585, Oak Ridge National Laboratory (1970).

INTERNAL DISTRIBUTION

1-3. L. S. Abbott
4. R. G. Alsmiller, Jr.
5. T. W. Armstrong
6. D. E. Bartine
7. A. A. Brooks
8. H. P. Carter
9. K. C. Chandler
10-19. R. L. Childs
20. C. E. Clifford
21. S. N. Cramer
22. N. F. Cross
23. M. B. Emmett
24. W. W. Engle, Jr.
25. G. F. Flanagan
26. W. E. Ford, III
27. T. A. Gabriel
28. N. M. Greene
29. W. O. Harms
30. O. W. Hermann
31. R. J. Hinton
32. J. R. Knight
33. J. L. Lucius
34. R. E. Maerker
35. F. C. Maienschein
36. B. J. McGregor
37. G. W. Morrison
38. F. R. Mynatt
39. P. Nelson
40. E. M. Oblow
41. J. V. Pace
42. S. K. Penny
43. L. M. Petrie
44. W. A. Rhoades
45. J. C. Robinson
46. R. W. Roussin
47. A. H. Snell
48. P. N. Stevens
49. J. G. Sullivan
50. D. K. Trubey
51. J. E. White
52. G. E. Whitesides
53. L. R. Williams
54. H. A. Wright
55. R. Q. Wright
56. A. Zucker
57. H. Feshbach (Consultant)
58. P. F. Fox (Consultant)
59. C. R. Mehl (Consultant)
60. H. T. Motz (Consultant)
61-62. Central Research Library
63. Document Reference Section
64-68. Laboratory Records
69. Laboratory Records - ORNL RC
70-79. Math. Division Library
80. ORNL Patent Office

EXTERNAL DISTRIBUTION

81. David S. Gabriel, Director, Division of Space Nuclear Systems, AEC, Washington, D. C. 20546

82. H. Goldstein, Room 242, Mudd Building, Columbia University, New York 27, New York

83. W. H. Hannum, Division of Reactor Development and Technology, AEC, Washington, D. C. 20546

84. P. B. Hemmig, Division of Reactor Development and Technology, AEC, Washington, D. C. 20546

85. Dr. V. A. Kamath, Scientific Advisor, Attn: P. K. Patwardhan, Bhabha Atomic Research Centre, Trombay, Bombay, India

86. Capt. Dean Kaul, Defense Nuclear Agency, Washington, D. C. 20305

87. K. O. Laughon, AEC Site Representative, ORNL

88. C. P. McCallum, Division of Space Nuclear Systems, AEC, Washington, D. C. 20546

89. P. F. Pasqua, Department of Nuclear Engineering, University of Tennessee, Knoxville, Tennessee

90. J. N. Rogers, Division 8321, Sandia Laboratories, P. O. Box 969, Livermore, California 94550

91. Dr. Milton E. Rose, Mathematics and Computer Branch, Division of Research, U. S. AEC, Washington, D. C. 20545

92-123. U. S. Atomic Energy Commission

124-125. Technical Information Center (TIC)

126. Research and Technical Support Division, ORO

127-163. Special NPD Distribution

OAK RIDGE NATIONAL LABORATORY
OPERATED BY
UNION CARBIDE CORPORATION
NUCLEAR DIVISION

POST OFFICE BOX X
OAK RIDGE, TENNESSEE 37830

SPECIAL 4TH CLASS RATE BOOKS

If a change of address is needed, indicate the change, include the zip code, and identify the document; tear off this cover and return it to the above address.